International Journal of Thermophysics, Vol. 26, No. 6, November 2005 (© 2005)
DOI: 10.1007/s10765-005-8598-z

Non-destructive Thermal Diagnostics of Porous Materials[1]

E. Litovsky,[2,3] S. Horodetsky,[2] and J. Kleiman[2]

Developed mathematical models of apparent thermal conductivity of porous materials are applied to non-destructive methods of thermal diagnostics. The non-destructive thermal diagnostics of porous materials can be used to estimate the size of pores and cracks in the range 10^{-9} to 10^{-3} m. A fractal model of porous structure and dependences of thermal conductivity/diffusivity on (experimental) gas pressure are used as a basis for structure parameter calculations. The measuring element (sensor) in this method is the mean free path of gas molecules in pores and cracks (Knudsen number) that is very sensitive to changes in gas pressure. Possible applications of the developed methods include non-destructive thermal diagnostics (NDTD) of nano- and micro-crack sizes; opening, closing and size changes of the cracks at high temperatures in a wide temperature range; evaluation of interfacial and contact heat barrier resistance for coatings; remote laser thermal diagnostics of the cracks; as well as obtaining data on strength, thermal shock behavior, failure and fatigue behavior of coatings and other structures. Examples of several applications of the NDTD method are presented.

KEY WORDS: gas pressure; materials; micro-cracks; nano-cracks; non-destructive; porous; thermal diagnostics.

1. INTRODUCTION

We would like to start the paper with a question: can thermal measurements be used to estimate geometric sizes? The logical answer could be: "In principle—yes, it is possible to calculate the thickness of a layer

[1]Invited paper presented at the Fifteenth Symposium on Themophysical Properties, June 22–27, 2003, Boulder, Colorado, U.S.A.

[2]Integrity Testing Laboratory Inc., 80 Esna Park Drive, Uuits 7–9, Markham, Ontario, L3R 2R7, Canada.

[3]To whom correspondence should be addressed. E-mail: elitovsky@itlinc.com

by measuring the thermal conductivity, dividing it by heat flux, and multiplying by temperature change." But the next question would be: "What for?" Such measurement would be much more complicated and less accurate than a measurement using a simple ruler or one of the modern techniques for thickness evaluation.

However, there are a number of cases where classical measurement methods give a large error, are very labor-consuming, and even impossible. Estimation of the porous structure parameters of a material is an example of such a case. It is related to the complicated stochastic microstructure, different shapes and sizes of pores, cracks, and different solid phases ranging from nano- to macro-scale. Preparation of thin micro- sections for microscopic investigations can destroy the real structure, including introduction of pores and cracks. Such methods as Hg porosimetry do not provide correct information about real pore size distribution since it measures the entry diameter of the pores, most of which have bottle-shaped contours.

The development and possible applications of a novel method of thermal diagnostics [1] of porous structures will be described in the present paper. The method is capable of estimating the geometric parameters of micro- and nano-cracks in a range of 0.5 nm to 100 μm, including evaluation of size distribution of the cracks and contact area between particles. The measured differences in thermal conductivity are indicative of changes in the solid phase, such as grain boundary segregation, dislocations, lattice defects in crystal materials, etc. [2–21]. Some of these issues will be discussed below.

We investigated thoroughly the correlations between the porous structure of materials, different heat transfer mechanisms, and apparent thermal conductivity/diffusivity [2–20]. The most recent results of our investigations have been published [10, 14, 15, 20], and the major conclusions from the above works can be summarized as follows:

(a) To understand the variations of thermal conductivity and diffusivity of ceramic materials that are caused by changing of the thermodynamic conditions, a thorough knowledge and proper characterization of material's geometry and composition is required. The material porosity and phase composition data only would not be enough. One should know the size distribution of pores and particles, the geometric parameters of contact heat barrier resistance (HBR), and the physical and chemical processes (segregation and diffusion, gas emission, opening and closing of micro-cracks) that may occur within the material.

(b) It is impossible to explain the complicated dependences of thermal conductivity, λ, on temperature and gas pressure, as observed in experiments by classical heat transfer mechanisms. The processes of conduction, convection, and radiation and the observed data are explained by several non-conventional heat transfer mechanisms, namely:

- Surface segregation and diffusion of impurities can explain the violation of the Eucken law in vacuum exhibited by λ of refractory metal oxides that contain fine pores (with diameter less than $1\,\mu m$) at the grain boundaries. The kinetics of the diffusion and segregation of impurities can affect reproducibility of the experimental data on λ in vacuum.
- Gas emission processes occurring in pores during fast heating of refractories govern the qualitative differences between pressure dependences of thermophysical properties measured by stationary and non-stationary methods.
- Non-uniform thermal expansion of grains in multiphase ceramics or in polycrystalline materials having anisotropic thermal expansion coefficient causes a change in geometric parameters of micro-cracks and, accordingly, affects the thermal conductivity.

The described models have several technological and metrological applications including selection of the reference data on thermophysical properties of porous ceramics; development of materials with predominant properties; understanding the reasons for poor reproducibility of experimental data and their scatter; and choosing standard specimens and measurement methods.

Developed theoretical models and adequate experimental thermophysical methods for characterization of porous structure and HBR of porous materials can be used in the method of thermal diagnostics. The method described in Ref. 1 found its first implementation in the estimation of average sizes of micro-cracks in plasma deposited alumina coatings [4]. A number of other possible applications of the NDTD method are discussed below, including measurement of distributions of geometric parameters of the cracks based on the fractal model of thermal conductivity.

We do not consider thermal diagnostics as a possible substitute for the direct methods, such as optical and electron microscopy, or some indirect classical measurement methods. An example of a classical indirect method for pore size distribution analysis is Hg porosimetry that is based on the model of Hg impregnation into cylindrical canals [22]. Evaluation of a spe-

cific surface is based on the model of mono- and multi-layer gas adsorption. A variety of models of particles sedimentation or models based on light/X-ray scattering are applied for analysis of particle sizes [22].

Our method also relates to the indirect measurement methods and requires application of some mathematical models that correlate material structure parameters and gas pressure in pores with thermal conductivity of materials. The method has a number of unique applications. However, it can be best used in combination with the classical methods. For example, microscopic methods are good for measurement of the distance between micro-cracks, sometimes for measurements of micro-crack thickness. Our method can additionally measure average sizes of the crack and contact area. The main benefit and unique feature of the NDTD method is the possibility of non-destructive measurements of structure parameters at high temperatures, including opening-closing of the cracks during heating-cooling of the materials, under thermal shocks, fatigue test, etc.

2. PHYSICAL BASIS AND MATHEMATICAL MODELS OF THE NDTD METHOD

For simplicity of the analysis, we will limit the number of the materials to those where influence of mass transfer mechanisms, including free gas convection, gas emission, and grain boundary segregation–diffusion are negligible [5, 6, 8, 20]. Examples of such materials include some sintered ceramics, refractories, composite materials, porous metals, ceramic coatings, etc. Models described below are more accurate when the porosity of the materials is less than 30–35%.

2.1. Measuring Micro-Element/Sensor

Gas pressure and apparent thermal conductivity measurements along with a mathematical model correlating the thermophysical properties and crack sizes provide sufficient information for evaluation of the geometric sizes of micro-cracks. The sensor used in our method is the same as in classical gas chromatographic chemical analysis [24] or in vacuum gas pressure sensors [24]—the thermal conductivity of the gas λ_g. Actually, λ_g is governed by the composition and the mean free path l of a gas molecule in the cracks/pores having a thickness, δ. In most cases the gas pressure inside pores is assumed to be equal to the pressure in a vacuum chamber where the apparent thermal conductivity is measured.

At pressures above atmospheric, the pore size normally greatly exceeds the molecular mean free path l, Knudsen number $Kn = l/\delta \ll 1$, and pore

thermal conductivity, $\lambda_{\Pi,g}$ is equal to the gas thermal conductivity, $\lambda_g(T)$. If the characteristic Knudsen number, as defined above, approaches or exceeds unity, one can define $\lambda_{\Pi,g}$ as a quantity dependent on the pore size. This is obtained using the expression for the heat flux through the layer of thickness δ filled with a gas at a pressure p [4, 5, 8, 10],

$$\lambda_{\Pi,g} = \lambda_g \left(1 + B \frac{p_{atm}}{p} Kn\right)^{-1} \tag{1}$$

where B is given by

$$B = \frac{4\gamma}{\gamma + 1} \frac{2 - A}{A} \frac{1}{Pr}. \tag{2}$$

Here γ is the specific heat ratio, Pr is the gas Prandtl number, and A is the accommodation coefficient. The accommodation coefficient A is defined as the ratio between the energy actually transferred by the gas molecules impinging onto a surface and the energy which could be transferred if these molecules reach thermal equilibrium at the surface. Bearing in mind that generally (i) the surfaces of polycrystalline solid materials in pores are rough and (ii) physical–chemical adsorption processes occur on the surfaces, one can take $A = 1$.

An example of a calculation of the relative thermal conductivity of a gap filled with air/nitrogen $\lambda_{\Pi,g}/\lambda_{g,\infty}$ is presented in Fig. 1 (as above $\lambda_{\Pi,g} = \lambda_g$, and other heat transfer mechanisms [14–16] are negligible). One can see that for sufficiently high pressures, or large pores (for which $Kn \ll 1$) heat transfer occurs in the continuum regime and $\lambda_{\Pi,g} \sim \lambda_{g,\infty}$, where $\lambda_{g,\infty}$ is the thermal conductivity of an "indefinite" gas layer.

$\lambda_{\Pi,g}$ decreases with decreasing p, especially in the transition and free-molecular regimes (where Kn may be comparable to 1). Estimates show that for a gap size δ of about 1 μm, $\lambda_{\Pi,g}$ decreases markedly with p,

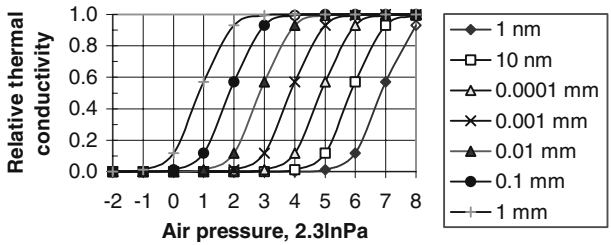

Fig. 1. Calculated plots of relative thermal conductivity of an air gap $\lambda_{\Pi,g}/\lambda_{g,\infty}$ versus the gas pressure, Pa, and thickness of the gap at 300 K.

decreasing below atmospheric pressure (10^5 Pa). For a 100 μm gap size $\lambda_{\Pi,g}$ starts to decrease significantly with gas pressure below $\sim 10^3$ Pa.

Fine-grained pure oxide materials are normally characterized by very small nanometer size pores, in which *Kn* reaches unity already at atmospheric pressure. For these materials Eq. (1) predicts a strong p-dependence of the effective thermal conductivity of the material λ_{eff} for higher pressures. This behavior might be important in super-insulating nano-materials.

The physical limitations of NDTD method applications depend on the effective diameter of the gas molecules. Nitrogen can be used in studies of pores/cracks with sizes larger than 5–10 nm. Helium allows studies of pores with sizes down to 0.7–1 nm. There are no physical limitations in evaluation of large sized pores/cracks when using the NDTD method. As can be seen from Fig. 1, by changing the gas pressure range, different pore thicknesses can be evaluated and measured.

Thus, at pressures of 10^6–10^7 Pa, nano-cracks; 10^3–10^5 Pa, micro-cracks; and 1–10^2 Pa, macro-cracks can be measured. A simple vacuum chamber with a roughing pump is sufficient for measurements of micro-cracks. A high-pressure chamber is needed for investigation of nano-cracks.

2.2. Correlations Between Structure Parameters and Apparent Thermal Conductivity

The effect of contact heat barrier resistances HBR on λ_{eff} is basically modeled [3–4, 10] by calculating the temperature field within two adjacent particles or grains, viewed as solid slabs with cross-sectional area πr^2 and contact area πa^2 (see Fig. 2). The external edge surfaces of the slabs are isothermal and the lateral faces are adiabatic. This model is aimed at calculating the effective thermal conductivity of a material composed of such contacting slabs, when a coarse-scale heat flux is applied in the x-direction (which is perpendicular to the cross-sectional area πr^2). The x-component, q_x, of this heat flux through this system may be expressed via the effective thermal conductivity, i.e., $q_x = -\lambda_{\text{eff}} \Delta T/L$, with the effective thermal conductivity of material λ_{eff} given by

$$\lambda_{\text{eff}} = \lambda_s M (1 - \Pi)^{3/2}, \tag{3}$$

where the HBR coefficient M may be calculated from the expression,

$$M = \frac{\frac{R_\Pi}{1-\bar{a}^2} + \frac{R_b}{\bar{a}^2} + \frac{\Phi^2}{\Phi - 1}}{\left(\frac{R_\Pi}{1-\bar{a}^2} + \frac{\Phi}{\Phi-1}\right)\left(\frac{R_b}{\bar{a}^2} + \Phi\right)}, \tag{4}$$

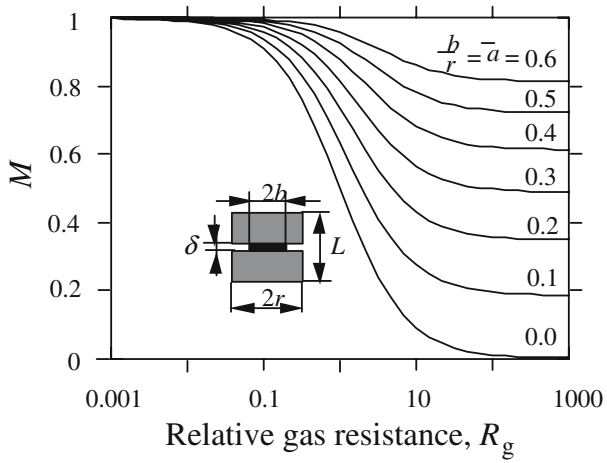

Fig. 2. Geometric model of heat barrier resistance together with the heat barrier resistance coefficient.

where

$$\Phi\bar{a}^2 = 1 - \frac{16}{\pi^2} \sum_{n=1,3,5,\ldots}^{\cdot} \frac{I_1(n\pi b/L)}{n^2 I_1(n\pi r/L)} \times [I_1(n\pi r/L)K_1(n\pi b/L) - K_1(n\pi r/L)I_1(n\pi b/L)].$$

In the above,

$$R_\Pi = \frac{\delta/\lambda_\Pi}{L/\lambda_s} = \frac{\lambda_s}{\lambda_\Pi}\frac{\delta}{L} \text{ and } R_b = \frac{\delta/\lambda_b}{L/\lambda_s} = \frac{\lambda_s}{\lambda_b}\frac{\delta}{L} \tag{5}$$

are the dimensionless thermal resistances of the crack and the contact layer of inter-grain material, respectively, where δ is the micro-crack thickness, L is the distance between the micro-cracks, b and r are the effective radii of the contact area and of the micro-crack (or grain boundary), $\bar{a} = b/r$, λ_b is the thermal conductivity of the inter-grain material, I_1 is the modified Bessel function of the first kind of order 1, and K_1 is the modified Bessel function of the second kind of order 1.

Usually R_b does not exceed 0.01, since $L/\delta > 100$ and λ_s and λ_b are of the same order of magnitude. For these values of R_b the HBR coefficient M does not depend upon the relative resistance of the contact spot and becomes a function of $\bar{a}^2$ and R_Π only. This function is plotted in Fig. 2. One can see that for $R_\Pi > 100$ (thick crack), M depends on the relative contact area only, and for $R_\Pi < 0.01$ (thin crack), $M = 1$. If $\bar{a}$ tends to 1,

M approaches 1 regardless of R_Π (here, pore thermal conductivity $\lambda_\Pi = \lambda_{\Pi,g} = \lambda_g$ also, and pore heat resistance $R_\Pi = R_g$).

If $Kn \ll 1$, the pore phase conductivity λ_Π is given by λ_g and is almost independent of gas pressure (see Fig. 1). In this case the gas thermal conductivity $R_g = R_\Pi$ is a function of δ/L and temperature. If $Kn \gg 1$ (low pressures, thin cracks), the heat flux across the crack is proportional to p.

2.3. Fractal Model of Microstructure of Porous Cracked Materials

The HBR phenomenon in ceramics and other materials arises from different technological and physico-chemical reasons in the course of material manufacturing and use. HBR normally is associated with discontinuities of different sizes, i.e., grain boundaries, cracks arising from pressing or kilning processes, practical use of materials, etc. Frequently the basic geometric structure of the discontinuities repeats itself on different length scales. Smaller scales describe structural elements of higher orders (or generations), for which elements are effectively included within the larger scale elements (of lower generations). Accordingly, a generalized geometric fractal model [4, 5] of the material microstructure has been proposed (see Fig. 3).

Consider a length scale (pertaining to a given generation) characterizing the average distance between the cracks, or a particle size. The length scales h_1, h_2 of 1 to 2 orders lie in the range of 1–10 mm. The length scale of third generation characterizes relatively large, sintered particles (grains) of the size 0.05–0.2 mm, separated by pores. The material grain boundary structure is governed by the binder character and the technological production process. The grain boundary may be composed of porous glass phase, chains of smaller pores, micro-cracks formed as a result of the material recrystallization and anisotropic thermal expansion of grains, etc. Structures of fourth (and higher-order) generations are characterized by low angle or, more frequently, large angle boundaries, and may also include networks of pores or submicro-cracks. The sizes of such boundaries are usually of the order 0.1–1 μm, and the corresponding pore sizes range from several Angstroms to 0.1 μm. Each i-th generation (length scale h_i) is characterized by its own grain contact area $\bar{a}_i^2$ and other pertinent parameters presented in Eqs. (3)–(5).

An expression for λ_{eff} of the above fractal, multi-generation porous medium may be obtained by repeatedly applying (at different length scales) the model of two slabs with HBR, described in the previous section. This is done by replacing the real structure by a model medium divided by grids of perpendicular planes—each having gap size

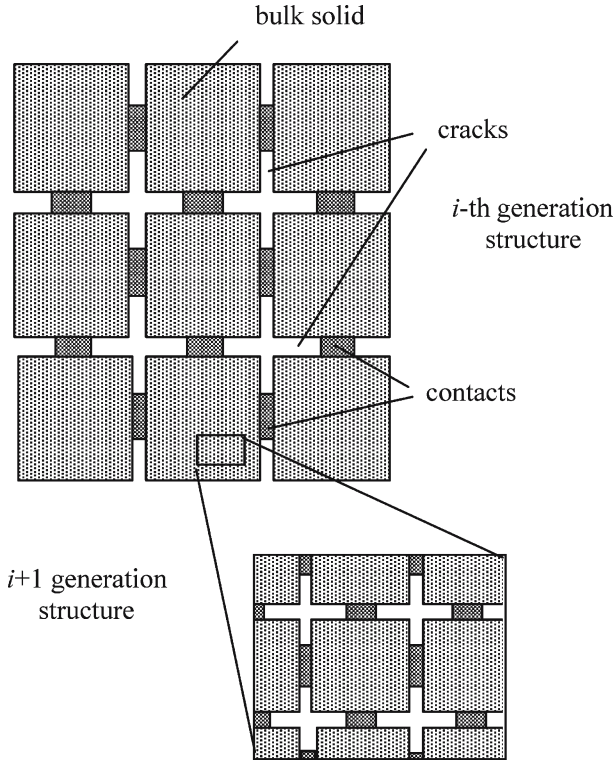

Fig. 3. Fractal model of porous materials.

h_i—corresponding to the size of a given generation in the real structure. The expression for λ_{eff} is [4]

$$\lambda_{\text{eff}} = \lambda_s (1 - \Pi)^{3/2} \prod_j M_j \tag{6}$$

where M_j is the HBR parameter of the jth-order structure.

3. POSSIBLE APPLICATIONS OF THE METHOD

It should be remembered that thermal diagnostics has been known for a long time, especially in solid-state physics. Development of the theory of phonon-mediated thermal conductivity and thermal capacity, evaluation of Debye temperature and lattice defects are connected with the names of A. Einstein, P. Debye, R. Peierls, A. Eucken, H. Casimir, P. Klemens, C. Kittel, etc., [21, 22, and references therein]. Our development

of thermal diagnostic methods deals mainly with the investigation of the porous structure and grain boundaries. The NDTD method is based on the measurement of thermal conductivity and diffusivity at different gas pressure/composition. This method can be best implemented for the measurement of geometric size distribution and average sizes of the micro- and nano-cracks.

Any methods for the measurement of thermal conductivity and diffusivity can be used in the NDTD method as a first stage of measurements. However, the number of the evaluated parameters and their accuracy will depend on the following experimental conditions:

- Maximum information and high accuracy can be attained when measuring the apparent/effective thermal conductivity at different gas pressures. Any additional information about porous structure should be useful, e.g., distance between cracks.
- Estimation measurements to assess and control the quality of products in industrial conditions can be conducted under the same gas pressure directly on the samples themselves or their parts, e.g., walls of buildings, turbine blades, electron chips, etc. Remote thermal diagnostics is most appropriate in this case.

Examples of different applications of the NDTD method are described below.

3.1. Structure of Cracks and Grain Boundaries

It is a tough experimental problem to measure the geometric parameters of thin cracks and grain boundaries, especially with sizes of nanoscale order. The optical and electron microscopic methods for characterization of micro-cracks and grain boundaries require the use of specially prepared cross-sectional samples. False porosity and micro cracks that can be introduced during the specimen preparation can misrepresent the real features of the porous structure. Evaluation of the average sizes of the cracks requires labor consuming statistical investigations.

The suggested method enables measurement of the average sizes of structural geometric elements that are needed for analyses of many technological and scientific problems . This is both the advantage of the method and sometimes its limitation.

Figures 4 and 5 present examples of calculations of the thermal conductivity of ceramic materials depending on gas pressure and the structural parameters using the fractal model. The ranges of the structure

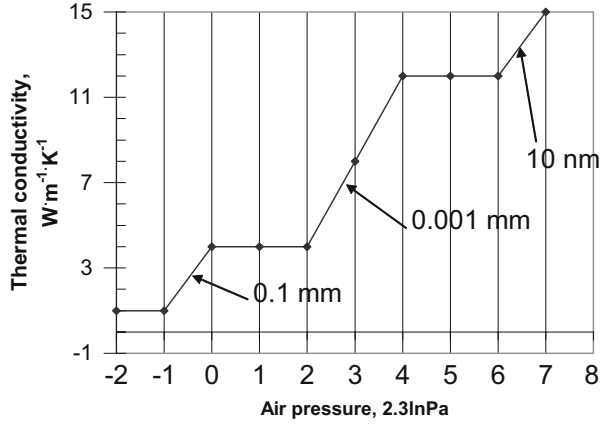

Fig. 4. Example of influence of gas pressure on apparent thermal conductivity of ceramics with cracks of different sizes.

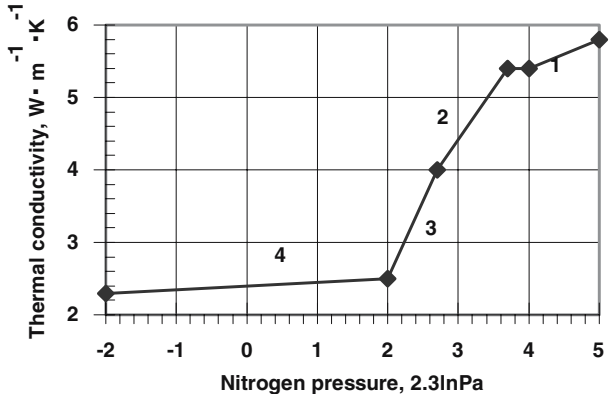

Fig. 5. Gas pressure dependence of thermal conductivity of magnesia ceramics at 400°C. The numerals (1–4) below and above the graph mark the segments with different structural parameters of the material as follows: 1. $\delta = 0.1\,\mu m$, $b/r = 0.7$ 2. $\delta = 1\,\mu m$, $b/r = 0.5$ 3. $\delta = 10\,\mu m$, $b/r = 0.4$ 4. $\delta = 0.2\,mm$, $b/r = 0.8$.

parameters summarized in Table I comply with the thermal conductivity data presented in Fig. 4.

The results of microstructure estimation for MgO, as shown in Fig. 5 by the NDTD method, are in accordance with the results of an analysis of the porous structure by optical microscopy and electron microscopy methods [23, 24]. Because it is very difficult to evaluate average parameters of

Table I. Possible Non-destructive Measurement Methods for Thermophysical Properties

#	Heat effect on the surface	Thermal conductivity	Thermal diffusivity	Thermal capacity	Thermal activity	Thermal radiation
1	Flash (heat pulse)	No	No	No	Possible	No
2	Constant heat flux	May be	No	No	Possible	Possible
3	Temperature waves, a change of temperature amplitude	No	No	No	Possible	No
4	Temperature waves, a change of temperature frequency (phase shift) and a change of temperature amplitude	Possible	Possible	Possible	Possible	Possible

contact area and thickness of the micro-cracks by microscopic methods, the comparison of results is only qualitative.

3.2. High Temperature Thermal Diagnostics

The suggested NDTD method has unique possibilities for analysis of porous structures at high temperatures. Micro-cracks exist between sintered grains in many refractories and ceramic materials. Some of these micro-cracks arise during the cooling stage after sintering of the material as a result of a mismatch in thermal expansion.

We developed a number of models aimed at investigation of the influence of opening and closing of micro-cracks on λ [10–12]. The models are based on the concept of thermal contact between the grains. This thermal contact may or may not exist in the absence of the mechanical contact. That is, even if a gap, ε, exists between the grains, they may be in thermal contact due to oscillations of the crystal lattice atoms. We assume that the bodies are in thermal contact, if $\varepsilon \cdot 5\,\text{Å}$, which is evaluated on the basis of solid-state physics [22, 23]. The micro-cracks can open and close during cooling–heating. The area and width of the micro-cracks depend on the temperature. The micro-cracks are open at temperatures $T < T_{\text{cl}} \cdot T_{\text{sin t}}$, where $T_{\text{sin t}}$ is the sintering temperature (about 1400–1600°C for many ceramics). At T_{cl} (temperature of closing), these micro-cracks are assumed to be closed [11, 12].

We described two possible modes of changes of geometric parameters of the micro-cracks with temperature [10–12]: (i) opening and closing of micro-cracks appearing around large grains, or (ii) opening and closing of micro-cracks within the bulk region.

In case of micro-cracks within the bulk region, the bulk region is viewed as consisting of small particles with small cracks between them

that arise due to thermal expansion mismatch. The average HBR parameters are calculated by integration over all particle sizes and their expansion coefficients. Using the above statistics of particle distribution, we obtain the contact area ratio and the average reciprocal crack thickness.

The calculated parameters $\overline{a}^2$ and δ^{-1} are used in Eqs. (4)–(7) to calculate the HBR parameter M and the effective thermal conductivity. In materials with coarse-grain structure, such as Al_2O_3 ceramics, chrome-magnesite refractories Radex E, Radex BC and fireclay refractories, HBR are formed by macro- and micro-cracks. Increase of λ with temperature in these materials can be attributed to the concomitant increase of the HBR parameter M, stemming from the increase of $\overline{a}$ and/or decrease of δ. In corundum this occurs as a result of the anisotropic thermal expansion of Al_2O_3 crystals [12]. The above mechanism explains the thermal conductivity data for several refractory materials for vacuum steel production, including Radex E, Radex BC, MCV, and MCVP [10–12].

The calculated values of the thermal conductivity along with the experimental data for the chrome–magnesite ceramics MCV are presented in Fig. 6. One can see that the model of reversible opening and closing of micro-cracks correlates well with the experimental data. The high closing temperature of micro-cracks explains the decreasing effect of the gas pressure on thermal conductivity with temperature. These investigations confirmed the applicability of high-temperature thermal diagnostics to the analysis of crack geometry at high temperatures.

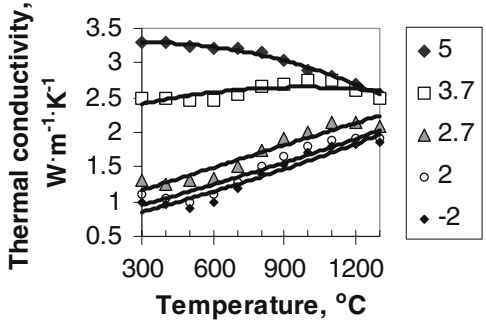

Fig. 6. Thermal conductivity of composite magnesia-cromite ceramics at different temperatures and gas pressure ($\log_{10}$ Pa). Solid lines are smoothed experimental data, symbols represent calculations [10].

3.3. Thermal Diagnostics of Mechanical Properties and Fatigue Failure

We found that good correlations between the mechanical and thermophysical properties exist for many dense and highly porous ceramic materials [2–3, 5, 13]. An example of thermal conductivity dependence on compressive strength of a porous MgO material is demonstrated in Fig. 7. The observed correlation can be explained by the fact that the same geometric structural elements like micro-cracks and grain boundaries govern both mechanical and thermophysical properties [2, 5]. As can be seen from this example, the method of nondestructive thermal diagnostics can be applied for control of mechanical properties.

We have applied the method of thermal diagnostics to control the fatigue behavior of metallic specimens that have been exposed to a complex loading that included a constant tension force along with a cyclic low frequency tension (5 Hz). The thermal diagnostics have been carried out by measuring the temperature difference dT at two points on the specimen (see Fig. 8), which was inversely proportional to the thermal conductivity of the specimen. The tensile stress has been monitored by a tensiometer (signal TNM in Fig. 8). One can see that the failure of the specimen has been registered by two methods simultaneously. A constant increase of the temperature difference (or decrease of thermal conductivity) during the initiation of the fatigue has been observed in the specimens. This effect can result from formation and accumulation of the lattice defects and processes of grain boundary segregation during mechanical treatment [21, 22].

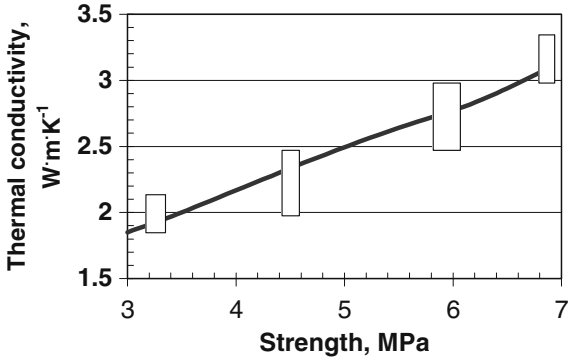

Fig. 7. Correlation between thermal conductivity of MgO ceramics and its strength; all specimens have the same porosity of 0.68 [13]. Squares represent the scatter of the experimental data. Solid line is the linear approximation.

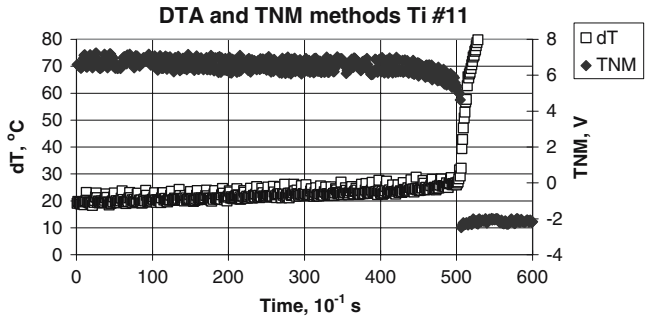

Fig. 8. Control of fatigue and failure of Ti specimen by tensiometer and method of thermal diagnostics.

3.4. Remote Thermal Diagnostics and Other Applications

Modern methods of laser and electron heating along with high-speed optical measurements enable development of remote measurement methods of thermophysical properties. The thermal-wave method provides more information than other known methods (see Table I) since it can utilize dependences between amplitude, phase, and frequency of the temperatures wave on the specimen surface [18, 19]. The change in thermal-wave frequency enables control of the wave's penetration/extinction depth and, as a result, estimates of the measurement depth of the cracks or other structural changes.

The method of temperature waves can be applied to characterize composition and structure of the underground layers in geological formations. Daily and seasonal temperature changes can be used for this purpose. Temperature wave distinction analysis has shown that seasonal temperature changes allow evaluation of the underground structure up to the depth of 10–20 m.

In the past decade, laser-induced thermal and acoustic transient methods attracted considerable attention in the context of the non-destructive characterization of properties of thin solid films and surface layers [25, 26]. Photothermal investigations are based on infrared photothermal radiometry. IR emissions are registered from the surface of the opaque material or even from the bulk, if the IR absorption coefficient is relatively low. The application of photothermal methods for investigation of thermal shock behavior of alumina ceramics has been demonstrated by Li et al. [26].

The transient grating technique which probes both acoustic and thermal responses of thin-film structures is suitable for mesuring mechanical

properies such as speed of sound, density, and elastic constants, as well as thermal properties. Examples of these applications can be found in the Proceedings of the Fifteenth Symposium on Thermophysical Properties [25].

4. CONCLUSIONS

1. A new non-destructive thermal diagnostic method has been developed.
2. The sensor in the method is the mean free path of gas molecules/gas pressure in pores and micro-cracks.
3. The method allows evaluation of average thickness and contact area of cracks and grain boundaries in the range of 10^{-9} to 10^{-3} m.
4. The fractal model of porous structure and measurement of the apparent thermal conductivity/diffusivity at different gas pressure enable to estimate the pore/cracks size distribution in the above range.
5. Different applications of the method have been demonstrated:
   - high-temperature structure diagnostics, including opening and closing of cracks;
   - analyses of the mechanical properties and fatigue;
   - remote control of the structure and mechanical properties.
6. Photothermal and acoustic transient methods are applied for non-destructive characterization of properties of thin solid films, surface layers, and bulk properties.

REFERENCES

1. E. Ya. Litovsky and U. P. Zarichniyak, *A Method for Measuring of Structure Parameters in Solid*, USSR Authorship N326498 (1978).
2. E. Ya. Litovsky, *J. Eng. Phys.* **6**:105 (1982).
3. E. Ya. Litovsky and M. Shapiro, in *Proc. 18*th *Int. Congress Theor. Appl. Mech.*, Haifa, Israel (1992), p. 95.
4. E. Ya. Litovsky, *Proc. Acad.Sci.USSR. Inorgan. Mater.* (1978), Vol. 14, pp. 1890–1894.
5. E. Ya. Litovsky and M. Shapiro, *J. Am. Ceram. Soc*. **12:**3425 (1992).
6. T. Gambaryan, E. Litovsky, and M. Shapiro, *Int. J. Heat Mass Transfer* **36:**4123 (1993).
7. T. Litovsky, R. Cytermann, E. Litovsky, M. Shapiro, and A. Shavit, *Advances in Porous Materials, Mater. Res. Soc. Proc*., S. Komarneni, D. M. Smith, and J. S. Beck, eds. (1995), Vol. 371, pp. 309–314.

8. E. Litovsky, M. Shapiro, and A. Shavit, *J. Am. Ceram. Soc*. **79/5:**1366 (1996).
9. E. Litovsky, T. Litovsky, M. Shapiro, and A. Shavit, *Third Symp. Insulation Materials: Testing and Applications, ASTM*, Quebec, Canada (1997), pp. 292–306.
10. E. Litovsky, T. Gambaryan-Roisman, M. Shapiro, and A. Shavit, *Trends in Heat, Mass and Momentum Transfer, Research Trends* (1997), Vol. 3, pp. 147–167.
11. E. Litovsky, T. Gambaryan-Roisman, M. Shapiro, and A. Shavit, presented at *24*th *Int. Therm. Cond. Conf.*, Pittsburgh, Pennsylvania (October 26–29, 1997).
12. E. Litovsky, T. Gambaryan-Roisman, M. Shapiro, and A. Shavit, *J. Am. Ceram. Soc*. **82:**994 (1999).
13. E. Litovsky, T. Litovsky, M. Shapiro, and A. Shavit, *Third Symp. on Insulation Materials: Testing and Applications, ASTM STP 1320*, R. S. Graves and R.R. Zarr, eds., Quebec, Canada (1997), pp. 292–306.
14. E. Litovsky, T. Gambaryan-Roisman, M. Shapiro, and A. Shavit, presented at *15*th *Euro. Conf. Thermophys. Props.*, Würzburg, Germany (September 5–9, 1999).
15. E. Litovsky, T. Gambaryan-Roisman, M. Shapiro and A. Shavit, *High Temp.-High Press.* **33:**27 (2001).
16. E. Litovsky and J. Kleiman, presented at 26th *Int. Therm. Cond. Conf.*, Boston, Massachusetts (2001).
17. E. Litovsky, J. Kleiman, and N. Menn, *Insulation Materials: Testing and Applications, ASTM STP 1426*, Vol. 4, A. O. Desjarlais and R. R. Zarr, eds. (American Society for Testing and Materials, ASTM International, West Conshohocken, Pennsylvania, 2002), pp. 257–269.
18. E. Litovsky, J. Kleiman, and N. Menn, *Protection of Materials and Structures from Space Environment, 6*th *Int. Conf*., Toronto, Canada (May 1–3, 2003).
19. E. Litovsky, S. Horodetsky, and J. Kleiman, presented at *Symp. Aerospace Materials: Development, Testing and Life Cycle Issues*, Montreal, Quebec, Canada (August 11–14, 2002).
20. E. Litovsky, J. Kleiman, and N. Menn, submitted to *High Temp.-High Press*.
21. T. Gambaryan, E. Litovsky, M. Shapiro, and A. Shavit, *Int. J. Heat Mass Transfer* **46/3**:385 (2003).
22. Charles Kittel, *Introduction to Solid State Physics*, Fourth Ed. (John Wiley, New York, 1978), pp. 211–249.
23. W. D. Kingery, *Introduction to Ceramics* (John Wiley, New York, 1967), pp. 300–331.
24. L. Hench and R. Gould, *Characterization of Ceramics* (Marcel Deccer, New York, 1971), pp. 219–271.
25. A. A. Maznev, presented at *Fifteenth Symposium on Thermophysical Properties*, Boulder, Colorado (June 22–27, 2003).
26. Bincheng Li, Andreas Mandelis, and Zoltan Z. Kish, *J. Appl. Phys.* **95:**1042 (2004).